Re-using Ladle Furnace Steel slags as filler in asphalt mixtures

Re-using Ladle Furnace Steel (LFS) slags as filler in asphalt mixtures

A. Roberto[a,*], L. Mantovani[b], E. Romeo[a], G. Tebaldi[a], A. Montepara[a], M. Tribaudino[b]

[a]*Department of Engineering and Architecture, University of Parma, Parco Area delle Scienze 181/A, Parma (Italy);*
[b]*Department of Chemistry, Life Sciences and Environmental Sustainability, University of Parma, Parco Area delle Scienze 157/A, Parma (Italy);*

Abstract

In the last few years, the deployment of the natural sources has been leading to re-use and recycle several materials that have been considered as "waste" so far. The proposed study analyses the possible re-employment of the Ladle Furnace Steel (LFS) slags as filler in hot mix asphalt (HMA) materials. Particularly, the main aim of the research is the evaluation of both the chemical composition of LFS and the performance level of HMAs. The analysis of the chemical composition was performed using the X-ray Fluorescence Spectrometry (XRF), the X-Ray Powder Diffraction (XRD), and the SEM-EDS Microscopy, involving three different hydration methods. The HMA performance level was evaluated at different scales (HMA, and mastic), using the SuperPave and the recently introduced Mastic Creep Tensile Tests (MTCT). The analysis involved three different conventional fillers and one type of LFS. Both HMAs and mastics were obtained using two asphalt binders (neat and 3.5% SBS polymer modified). In terms of mechanical characterization, the results showed an increased level of the brittleness of materials containing LFS. While, the LFS chemical and mineral composition does not exhibit significant changes, even though, after LFS hydration, a small new peak was highlighted by the XRD analysis.

Keywords: Steel slags; Resource efficiency; Asphalt mixtures; Circular economy; Waste management; Hydration effects;

1. Introduction

Nowadays the amount of steel and iron is increased up to 147 054 thousands tonnes [1], and its production outputs are characterised by 64.4% of steel, 32.9% of so-called "*by-products*" and 2.7% of wastes. Basically, steel-making operations is distinguished by the type of furnaces: Basic Oxygen Furnace (BOF); Eletrical Arc Furnace (EAF); Ladle Furnace (LF). The necessity to move towards the circular economy has been requiring the possibility of reusing steel disposed by-products, which are not considered wastes since September 1995 [2].

Steel slags are produced during the final stages of steel production, adding quicklime to the heated-steel coming from the furnace. Through this addition, the material is subjected to several phisico-chemical processes (such as desulfurization, degassing of oxygen, nitrogen, and hydrogen, removal of impurities, and final decarbonization), which is well known as refining operation [3].

In the last few years, the use of LFS has been spreading in different fields such as road application [2, 4], soil stabilization [3], earthwork and armourstones for hydraulic structures [2].

Generally, the steel production is a batch process in which the chemical reactions are not ended [5], thereby LFS composition is characterised by silicates and aluminates of calcium and magnesium [3]. Their content is non-uniform [5] and both the free-calcium oxide (CaO) and magnesium oxide (MgO), among others, generally represent 50-60% of the total weight of LFSs [3, 5, 6], which is strictly furnace-type-dependent [7]. The material's composition is also distinguished by a CaO/SiO_2 equal to 2 [8]. LFS are characterised by their own gradation curve with a maximum size up to 1-2 mm [4, 9, 10], high porosity (Rigden voids [11] approximately 40% [4]) and particle density level (from 2.8 g/cm^3 [9] to 3.2 g/cm^3 [4]).

Flexible pavements are composed by different overlapped layers, each serving a specific function. The binder layer is the one that performs the most structural service. The binder layer typically is composed of aggregates, asphalt binder and filler, which is the fine por-

*Corresponding author.
Email address: antonio.roberto@unipr.it (A. Roberto)

tion of aggregates smaller than 0.075 mm in size. LFS may be used as a filler in the HMA.

Currently, the LFS content is limited due to the following problems: volumetric instability and expansion connected to the miscellaneous chemical composition which is extremely H_2O and CO_2 reactive [3, 5], hydration and carbonation phenomena, respectively; bitumen absorption linked to the high porosity of the material [4, 9, 10]; less workability and compaction of the mixtures containing LFS [4, 12]; and, leaching problems [4]. These are all linked each other.

Basically, the hydration is probably the most important problem due to the long lasting aptitude required to the asphalt mixtures. In fact, if the hydration phenomenon is not completed, it can generate swelling problems for both bounded and unbounded layers [2].

The hydration process basically starts from the stoke procedure (stockpile or silo) of steel slags due to weathering conditions [13], concerning primarily the CaO and MgO.

Ortega-López et al. [3] distinguished two different kinds of free-CaO morphologies, "*primary*" and "*secondary*" CaO, and one of free-MgO in the LFS composition. Both of the them are important in the liquid phase (at high temperature) to protect the refractory wall of the furnace.

The CaO hydration process allows to obtain the $Ca(OH)_2$, which is characterised by a higher density than the CaO. This means that the chemical instability, combined with the hydration phenomenon, leads to an increased material volume (swelling up to 100%), and this effect is higher for vapour-using procedures [14]. This process generally finishes in few days if water access is allowed [7].

The free-MgO is characterised by a slow hydration, and it can last for many years producing the increase of volume [7]. The presence of this compound is quite difficult to be estimated and cannot be evaluated by chemical analysis, thereby only the X-ray diffraction gives a semi-quantitative estimation. Considering the long-term swelling, the free-MgO is able to produce volumetric expansion computable with a factor from 2 to 10 [3].

Important consequences of these complex chemical reactions are also linked to the carbonation. This complex phenomenon allows to find $CaCO_3$ (calcite and vaterite) [6] and $MgCa(CO_3)_2$ (dolomite) [7] in the LFS dust without significant swelling problems.

Due to the complexity of the chemical interaction and reaction, it is not easy to establish *a priori* the volumetric expansion [3]. Several studies [3, 4, 6, 15, 16] were focussed on the evaluation of the hydration phenomenon and its consequences, but the use of LFS still needs caution [10]. Therefore, other studies were focussed on the possibility of limiting the CaO and MgO effects through the modification of the cooling system of the liquid slag [13] or by creating a protective bituminous coverage of the LFS particles [10]. Choi et al. [13] evaluated the possibility of avoiding the presence of both free-CaO and -MgO, modifying the production chain of steel-making-plants.

The employment of LFS in Hot Mix Asphalt (HMA) can cause high bitumen absorption and decreased workability. These are mainly linked to the high porosity of the material and the bitumen-LFS interaction. Several studies [4, 10, 17, 18] investigated these specific effects. Skaf et al. [10] demonstrated the good LFSs' adhesion with bitumen, highlighting the quality of the formed mastic. Nevertheless, the interaction between LFS and bitumen increases the viscosity and the stiffness of mastics [9]. Thus, the decreased workability of HMAs reduces the material compactability [19], leading to high air-void content of final mixtures [4].

Nevertheless, the rutting performance increases when the LFS are included as filler into the mixtures. Basically, the porous structure of LFS seems to increase the shear resistance by absorbing the extensive oil which causes the permanent deformation at high temperatures [17].

Generally, HMAs containing LFS show improvements in the Indirect Tensile Strength (ITS), resilient modulus, rutting resistance, fatigue life, creep modulus, and stripping resistance [18]. Nevertheless, the increase in tensile strength leads also to brittle phenomenon as remarked by Pasquini et al. [19].

2. Objective and scope

This study aims at investigating the feasibility of using LFS as filler in the HMA, in order to enhance the sustainable level of road infrastructures.

The study proposed is based on the chemical evaluation of LFSs and the mechanical characterization ofasphalt materials (HMAs and mastics), considering both hydrated- and not hydrated-LFSs.

In particular, due to the time-dependency of the hydration process [3, 7, 13], its effects were evaluated involving three different times (48 hours, 7 days, and 15 days), and using three different hydration conditions indicated as weathering [13], 0.32 [4], and 2. The first one requires only to expose the LFS to the air moisture, while the others are based on the H_2O/CaO ratio. Those processes are further indicated as ageing process.

The chemical analysis was performed using the XRF, the XRD, and the SEM-EDS. The mechanical behaviour of the mastic (asphalt binder + filler) and the HMA was evaluated using the MTCT [20] and the SuperPave protocol [21–24], respectively.

Both mastics and mixtures were then compared with a reference HMA containing only virgin aggregates and three different fillers, one limestone (L) and two limestone + 20% hydrated lime (A and F), which are typically used for the asphalt pavement layer considered (binder).

3. Materials and methods

3.1. Asphalt binders and fillers

The study herein involved two asphalt binders, one Neat (N) and one SBS Modified (M) (containing 3.5% of cross-linked SBS polymers), limestone aggregates and filler, and one type of LFS slags.

The asphalt binders are both commercial and characterised by Performance Grade (PG), which is 58-22 and 64-22 for the N and M, respectively. This parameter describes the expected performance level of asphalt binders, considering the service temperatures.

It is worth to remark that filler, in this case of study, indicates the aggregates distinguished by a grain-size up to 0.075 mm. Thus, the involved materials were sieved before preparing the analysed specimens.

The filler used are the L, A and F, which were used as reference, and LFS. Particularly, A and F, which contain 20% hydrated lime, are characterised by two different hydrated lime types which differ in Specific Surface Area (SSA), high and standard, respectively.

3.2. Ageing process for LFS materials

As mentioned above, the hydration process of the LFS is often labelled as the ageing process of the material [13]. As widely demonstrated by several authors [3, 4, 10, 12, 19, 25], this process is furnace-dependent, and can start during the storage (stockpile or silo) and lasts for many years. For the proposed case of study, the ageing process is characterised by three hydration conditions, and each one of them was combined with three different durations.

The times involved were: 48 hours; 7 days; and 15 days. Those were used to select the proper and faster process to age the LFS.

The selected hydration conditions were:

- the weathering process, which is based on exposing the LFS to the air moisture;
- the partial immersion, which is characterised by a H_2O/CaO ratio equal to 0.32. This procedure is based on partially immersing the LFS into a water-bath.
- full immersion, which is distinguished by a H_2O/CaO ratio equal to 2. This procedure is based on fully immersing the LFS into a water-bath.

Each one of the combined-ageing procedure was ended by drying the LFS. This was performed at 105°C continuously monitoring the mass of the LFS until it became constant.

3.3. XRF analysis

The bulk composition was measured by means of X-ray fluorescence spectrometry (XRF). About 3 g of the dried and milled material was used. Before analysis, each sample was first pressed in a boric acid binder to obtain a thinlayer pressed powder pellet (37 mm in diameter). A sequential wavelength dispersive Xray fluorescence (XRF) spectrometer (Axios-Panalytical), equipped with a 4 kW Rh tube and SuperQ 3.0 software, was used. The estimated precision for elemental determinations is higher than 0.5% for all elements.

3.4. XRD analysis

The X-ray powder diffraction was performed using a Bruker D2 PHASER diffractometer (Bruker, Karlsruhe, Germany) equipped with an Si(Li) solid state detector. Intensity measurements were run at 30 kV and 10 mA and were taken using CuKa radiation (lambda = 1.54178 Å) in steps of 0.02° over a 2theta range from 6° to 70°, with a counting time of 2 s per step. The identification of the phases was performed with the EVA software (Bruker), and COD database (Crystallography Open Database).

3.5. SEM-EDS Microscopy analyses

The samples were examined with a SEM-EDS Jeol 6400 Scanning Electron Microscope equipped with an Oxford EDS (Energy Dispersive System) microprobe. Microprobe analysis operating conditions were 20 kV and 1.2 mA current, 1 mm beam diameter and 75 s counting time; 15 analytical points per sample were taken. The powder samples were deposited on a graphite layer and covered with a high-conductance thin graphite film to avoid charging effects. SEM images were obtained using back-scattered electron detector, to better assess the presence of composition heterogeneities or discriminate different phases in the samples.

3.6. The MTCT

The MTCT was recently introduced by Roberto et al. [20] to analyse the creep behaviour of mastics in the small-strain domain (linear-viscoelasticity). Considering those conditions, the creep behaviour of bituminous materials can be divided in three phases [26]. Particularly, this study is focussed on the first two, the primary creep and the secondary stage.

This method is based on testing dog-bone shaped samples under an uniaxial tensile load ($P = 60\ N$). The creep behaviour is described by two parameters indicated as creep compliance J and *m-value*. Whilst, the first one is the strain per unit of applied stress [26], the second one indicates the strain accumulation rate.

J is calculated as follow:

$$J = \frac{\varepsilon_{180}}{\sigma} \qquad (1/MPa) \tag{1}$$

where ε_{180} is the measured deformation after 180 seconds, $\sigma = P/A$ is the stress due to the tensile load P, and A is the area of the cross-section of the sample (200 mm^2).

While, the *m-value* is calculated by fitting the $J(t) -$ *curve* (creep curve) using the Power model 2.

$$D(t) = D_0 + D_1 t^m \tag{2}$$

Where $D(t)$ is the creep compliance at time t, D_0 describes the instantaneous elastic response of the materials, D_1 is the parameter linked to the long-term, and m is the m-value.

3.7. SuperPave IDT test

The SuperPave IDT [21–23] is a performance-related test which allows to characterise the fracture/strength behaviour of the HMA. The procedure requires to test the materials at 10 °C using the indirect tension configuration.

The materials' behaviour is described through three parameters, the Resilient Modulus (M_R) [21], the creep compliance ($D(t)$) [22], and the Tensile Strength (S_t) [23]. Those parameters allow to interpret the elastic response of the materials, the HMA proneness to accumulate permanent deformation, and the resistance of the materials up to the first-fracture [23].

3.8. SuperPave IDT specimen preparation

The HMA SuperPave IDT specimens are cylindrical specimens, 150 mm in diameter and 35 mm in thickness (further indicates as HMA specimens). To better understand the role of fillers on the HMA fracture resistance, the same virgin-grading curve, considering a 12.5-mm-nominal aggregate maximum size, and asphalt binder content (5.2% by the weight of the aggregates) were used for all of the analysed HMAs. The specimen preparation procedure is based on the protocol developed by Cominsky et al. [27]. By following this procedure, two 4500-grams batches of virgin aggregates were prepared for each filler used. Consequently, they were placed in a draft oven at equiviscous temperatures (160°C and 170°C for the N and M, respectively) for four hours before mixing. A pre-heating phase was also required for the N and M asphalt binders (5.2% by the weight of aggregates), which were heated at least one hour. Successively, pre-heated materials were mixed. The obtained HMAs were aged, as provided by the SuperPave procedure for two-hours at 135°C. After the ageing period, the materials were compacted by using a gyratory compactor, applying 126 gyrations, which allowed to achieve 6% (± 0.5%) air void. The 4500-g-cylindrical specimen were allowed to cool down for at least 12 hours, and, successively, were firstly trimmed, removing the top and the bottom part for reducing the density gradient effects, and consequently sawn to obtain two 30-mm-thick-circular shaped specimens. The obtained HMA samples were then tested following the SuperPave procedures at 10°C.

3.9. Mastic specimen preparation

The mastic specimen preparation followed the methodology introduced by Roberto et al. [20] which involves two phases: pre-heating and mixing. During the first one, both asphalt binders and fillers were allowed to heat at equiviscous temperature (160°C and 170°C for the N and M, respectively), as already described for the HMA specimen preparation. The fillers were pre-heated for four hours, while the asphalt binders were heated for at least one hour.

Successively, the mixing operation was performed by using a high-share mixer. The procedure establishes,firstly, to place the asphalt binder in a 500-ml-pot, and, secondly, to add the fillers to the melted bitumen, which are roughly mixed. Only when the filler is fully immersed in the bitumen, the mechanical mixing procedure starts up to achieve the maximum rotation (7000 rpm) which is kept for 90-seconds [20, 28].

The obtained materials were then poured in the dog-bone-shaped-moulds [29], which were successively allowed to cool down for 12 hours. After cooling, the specimens were stored for 4 hours at 7°C, which is the testing temperature. The specimens were all prepared considering a binder/filler ratio equal to 1.5, referring at the HMA described above.

4. Results and discussion

4.1. Chemical composition

The chemical composition was determined to establish the CaO/H_2O. The results of the XRF are shown in Table 1, as g of oxides/100g of material (wt%). As noticeable, the main composition of the bulk material is characterised by the presence of CaO (54 wt%), SiO_2 (23 wt%), MgO (13 wt%), and Al_2O_3 (7 wt%) compounds, as expected.

XRD results. The XRD analysis of the LFS can be split in two parts: the first one is focussed on the mineralogical composition of the bulk material (as received) while the second one is the comparison among the three-different hydrated methods and the bulk material.

The XRD pattern is reported in Figure 1. Due to the important problems linked to the LFS use described above, the identification of mineralogical phases is done not only in order to recognize the major phases but also to characterize the presence of water sensitive mineralogical compounds.

The main phases detected are orthorhombic and monoclinic calcium silicate (Ca_2SiO_4), called as γ-C_2S and β-C_2S respectively, periclase (MgO), cuspidine ($Ca_4Si_2O_7F_2$), and cacium aluminium oxide fluoride ($Ca_{12}Al_{14}O_{32}F_2$), merwinite ($Ca_3MgSi_2O_8$) and melilites $Ca_2M(XSiO_7)$ with M = Mg, Al, and X = Si, Al. Minor phases are represented by fluorite CaF_2, portlandite $Ca(OH)_2$ and probably aluminum hydroxide and alumo-silicates. Moreover, amorphous material is also present. As not expected, none CaO main peaks were detected (Figure 1). Nevertheless, the presence of $Ca(OH)_2$ was highlighted, indicating that CaO had likely hydrated during either the production or the storage period. This leads to the assumption that the hydration of the CaO is quickly ended due to the fineness of the LFS grains. The major and minor mineralogical phases are summarized in Table 2.

The results of the comparative analysis among the bulk and hydrated materials are shown in Figure 2. In detail, considering the XRD spectra drawn in Figure 2a, the analysis of single hydration method and its durations can be reported.

Analysing the weathering method, the three durations, represented by 48 hours, 7 and 15 days do not show significant differences. Indeed, the weathering pattern are all characterized by the strong periclase (MgO) peak highlighted by the green-dashed rectangle (Figure 2a), and by the same mineralogical phases found in bulk material. This indicates that no-changes in the mineral composition are remarked among the bulk and weathering- aged materials.

Analysing the model of the aged LFS using 0.32 as CaO/H_2O, it can be observed that, at atmospheric conditions, there is no variation for all three durations used. Nevertheless, by comparing the 0.32-spectra with the bulk one, a new small peak is found at 10.6 2theta (red-dashed-rectangle). This was also observed for the spectra of aged materials having 2 as CaO/H_2O (Figure 2a) where the peak increases in intensity. Due to this XRD-assessment, and to ensure a fairly good LFS hydration condition, henceforth, the study refers to 48-hour-full-immersed material (CaO/H_2O = 2) as the best method for hydrating the LFS. Many attempts have been made to identify the newly formed phase but, for now, only assumptions can be made suggesting hydrated calcium aluminate, partly because of the location of the low-2θ peaks, probably characterized by a large unit cell phase.

SEM-EDS results. To investigate both the morphology and the composition of each sample, SEM-EDS analysis was performed on wathered powder samples. In terms of particle size and morphology, no differences were observed among the three treatments. The material, previously sieved at 75 microns, shows a particle size ranging from a few microns, that represents the lower resolution limit of the instrument, to 100 microns. Few grains greater than 75 microns were found, almost all elongated, probably passed through the sieve. A chemical map and an accurate morphology observation of the bulk material was also made and shown in Figure 3. The morphology of the bulk sample is similar to that of weathered ones, but larger particles are observed as the sample is not sieved. The chemical map confirms and supports the XRF results: the major elements are represented by Ca, Si, Mg and Al. Therefore, a good percentage of F and S is present. In general, most of the powder is calcium silicates, thus confirming the XRD analyses on the presence of C_2S. Calcium aluminates, periclase and crystals with F are also evident, supporting the presence of F-bearing mineral phases. Some grains with S, not found at XRD, have been seen here, probably as alteration products.

4.2. LFS effects on HMA properties

As results of the chemical composition above discussed, the LFS, bulk and hydrated, were compared with three conventional fillers. These were then mixed with the N and M asphalt binders to obtain both HMAs and mastics. The label used for the materials following described are all summarised in Table 3.

Table 1. XRF results for the bulk sample analysis. The elements are expressed as g of oxides/100 g of material (wt%)

Oxidation	CaO	SiO_2	MgO	Al_2O_3	P_2O_5	Cr_2O_3	K_2O	Na2O	MnO	TiO_2	Fe_{tot}	FeO	S
wt%	53.40	23.20	12.90	6.70	0.01	0.01	0.02	0.02	0.50	0.50	0.70	0.90	1.10

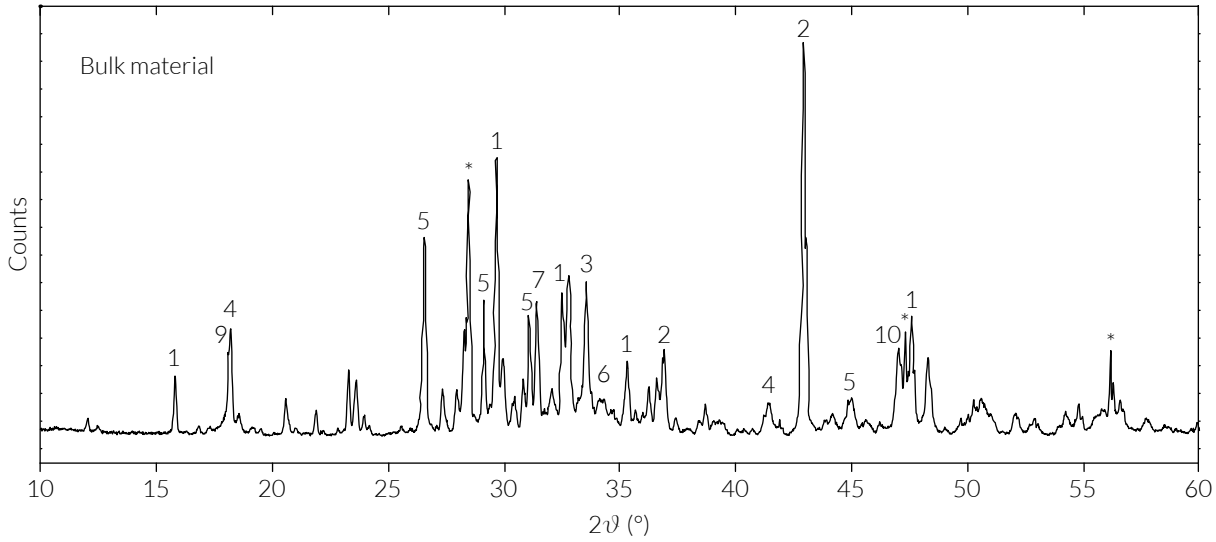

Figure 1. The XRD spectrum of the bulk material as received.

Table 2. Mineralogical phases of the bulk material.

Label	Name	Chemical formula	Mineral name
1	*Calcium Silicate*	$Ca_2(SiO_4)$	gamma-C_2S
2	*Magnesium Oxide*	MgO	Periclase
3	*Calcium Magnesium Silicate*	$Ca_5MgSi_3O_{12}$	–
4	*Calcium Aluminum Oxide Fluoride*	$Ca_{12}Al_{14}O_{32}F_2$	–
5	*Calcium Fluoride Silicate*	$Ca_4Si_2O_7F_2$	Cuspidine
6	*Calcium Silicate*	Ca_2SiO_4	Larnite
7	*Calcium Aluminum Silicate*	$Ca_2M(XSiO_7)$ with M = Mg, Al, and X = Si, Al	Melilite
8	*Aluminum Hydroxide*	$Al(OH)_3$	Nordstrandite
9	*Calcium Hydroxide*	$Ca(OH)_2$	Portlandite
10	*Calcium Fluoride*	CaF_2	Fluorite
*	*Silicium (Standard)*	Si	–

MTCT results. The analysis of mastics was performed using the MTCT developed by Roberto et al. [20]. The results were obtained applying a 60-N-constant load for a loading period of 180 seconds. The test was performed at 7°C to assure a visco-elastic behaviour of the mastic. Moreover, the deformation of the material are in the small-strain-domain. The material creep behaviour was investigated in terms of accumulation of permanent deformation (strain curve), creep compliance (J_{MTCT}), and m-value. The results are all collected in Figure 4.

The strain curves are drawn in both Figure 4a and Figure 4b for the N and M series, respectively. The main difference between the N- and M-base materials is the smoothness of the strain curves referred to the M-series, as expected. This is mainly due to the polymer contained in the M-asphalt binder, which collaborates to reduce the permanent deformation [30]. Despite this important difference among the analysed data, the bitumen-filler reaction are evident for both the N- and M-series. In fact, by looking at Figure 4a and Figure

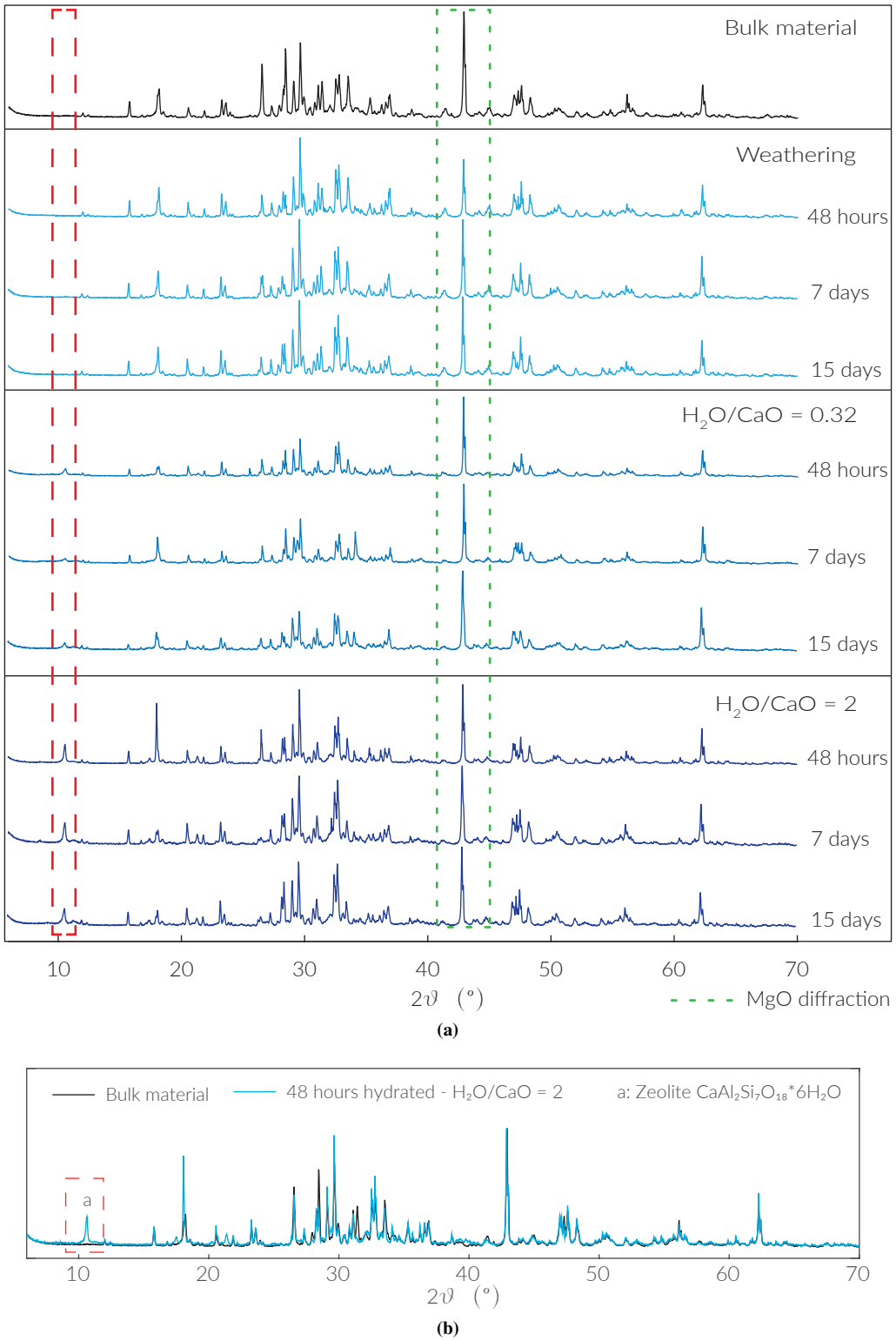

Figure 2. Comparison among the bulk material and the several hydration methods (**a**), highlighting the differences between bulk and 48-hour-full-immersed material (**b**) in terms of XRD diffraction.

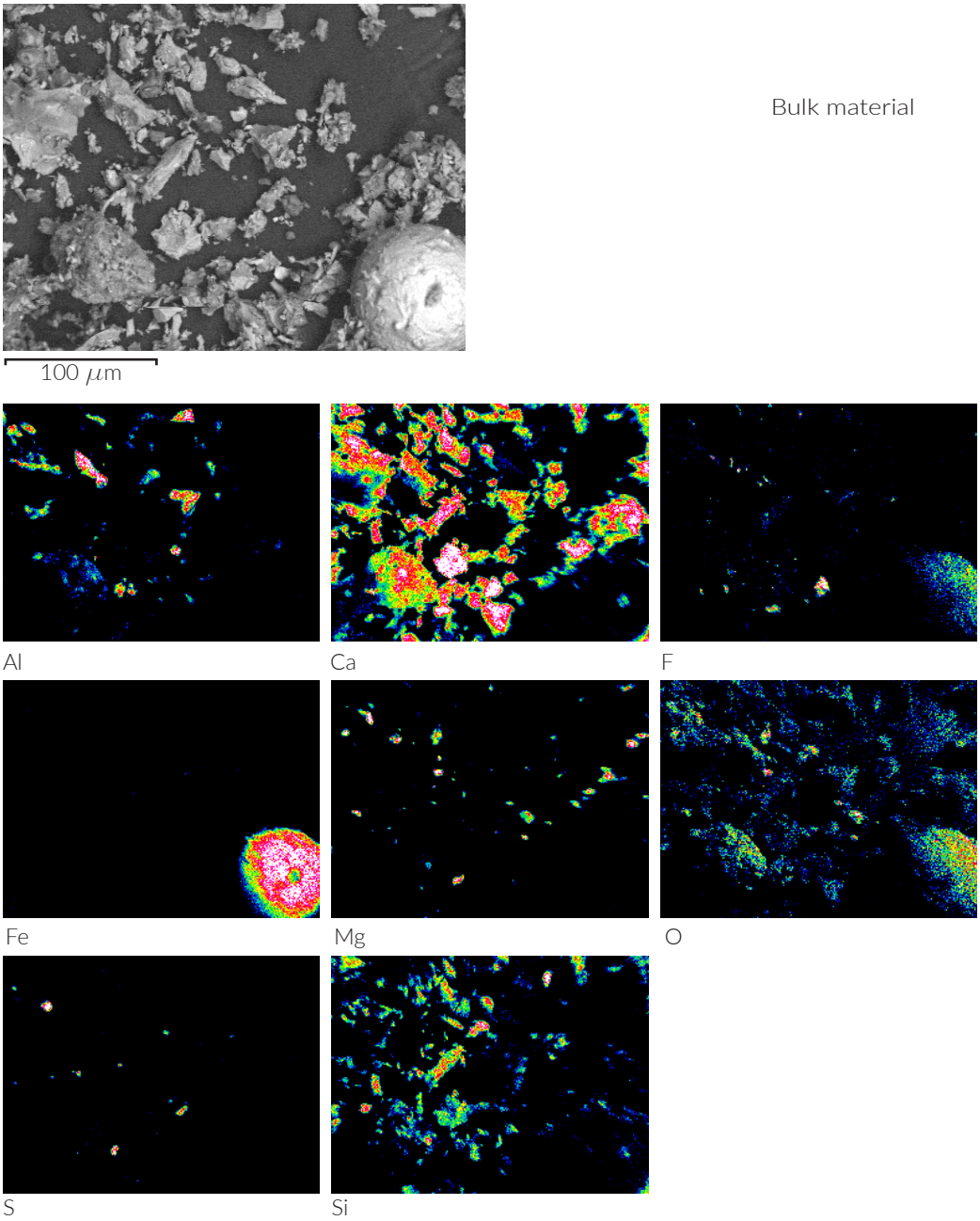

Figure 3. SEM-EDS analysis of the bulk material showing the distribution of the main chemical elements found.

Table 3. Summary of the used labels for indicating the tested materials.

Asphalt binder	Asphalt binder label	Filler	Filler label	Material label
SBS Modified	M	Limestone	L	*ML*
SBS Modified	M	Limestone + Hydrated lime*	A	*MA*
SBS Modified	M	Limestone + Hydrated lime**	F	*MF*
SBS Modified	M	LFS not hydrated	SNH	*MSNH*
SBS Modified	M	LFS Hydrated***	SH	*MSH*
Neat	N	Limestone	L	*NL*
Neat	N	Limestone + Hydrated lime*	A	*NA*
Neat	N	Limestone + Hydrated lime**	F	*NF*
Neat	N	LFS not hydrated	SNH	*NSNH*
Neat	N	LFS Hydrated***	SH	*NSH*

* 20% of high SSA hydrated lime.

** 20% of standard hydrated lime.

*** LFS hydrated for 48 hours into a water bath.

4b, the gap between the conventional fillers and LFS, bulk and hydrated, is remarkable. This effects is likely linked to the high quantity of hydrated-lime in the LFS, especially for the hydrated condition which stiffens the mastics [29, 31, 32].

By focussing on the J_{MTCT} results (Figure 4c), the differences highlighted above are also confirmed. However, the J_{MTCT} is not able to remark the differences among the Neat and SBS modified series. This is probably linked to the quite similar properties (Performance Grades) of the used asphalt binders.

Conversely, the m-value, which describes the accumulation rate of the deformation, seems to be asphalt-binder-nature sensitive, as shown by Büchner et al. [33], who indicate the creep rate (m-value) as a material property for the creep behaviour evaluation. The collected results highlighted that the LFS are able to stiffen the mastics, as already discussed for the strain curve analysis.

Basically, the analysis proposed does not highlight differences among the materials containing LFS as-received (bulk) and hydrated, especially when they are combined with the M asphalt binder.

HMA mechanical properties. The HMA analysis was carried out performing the SuperPave protocol at 10°C. The mechanical properties of the HMAs are expressed in terms of M_R, D(t), m-value, S_t, and ε_f, ad are summarised in Table4.

Looking at the M_R results, it can be remarked that the elastic response of the HMAs is quite similar for all of the analysed fillers, as expected. The MR is closely related to the lithic skeleton of the specimen, and, in this study, all mixtures are characterized by the same aggregate curve.

In terms of creep behaviour, despite the creep phenomenon is mainly linked to the asphalt binder nature, the D(t) analysis highlighted that the proneness to accumulate permanent deformation is reduced when the fillers containing hydrated lime, and NSH filler are used. This was observed for both the asphalt binders involved. However, the analysis of m-values remarks a lower creep-rate for the HMAs prepared using the SBS modified asphalt binder, as expected.

The analysis of the mechanical properties at first fracture, S_t and ε_f, highlighted the important role of the filler-bitumen reactions [11, 29, 31, 32, 34, 35]. In fact, observing the materials prepared with the M-bitumen, the HMAs containing hydrated lime exhibited higher S_t and ε_f, while both MSNHs and MSHs show an acceptable S_t, and a lower ε_f. This indicates that both SNH and SH fillers stiffen the HMAs, leading to a more brittle behaviour. The same consideration can be done for the materials containing the N-bitumen, but, in this case, the results indicate that the stiffening effect is much higher when the SNH is used.

Summarising, the M_R, D(t), and S_t are generally not affected by the filler nature, while the deformability of the HMAs is widely filler dependent. Actually, the SH and SNH are able to highly stiffen the HMAs, affecting both the m-value (creep rate) and the ε_f.

5. Summary and conclusions

The study herein is part of a wide research project, which aims at evaluating the use of the LFS, a waste ma-

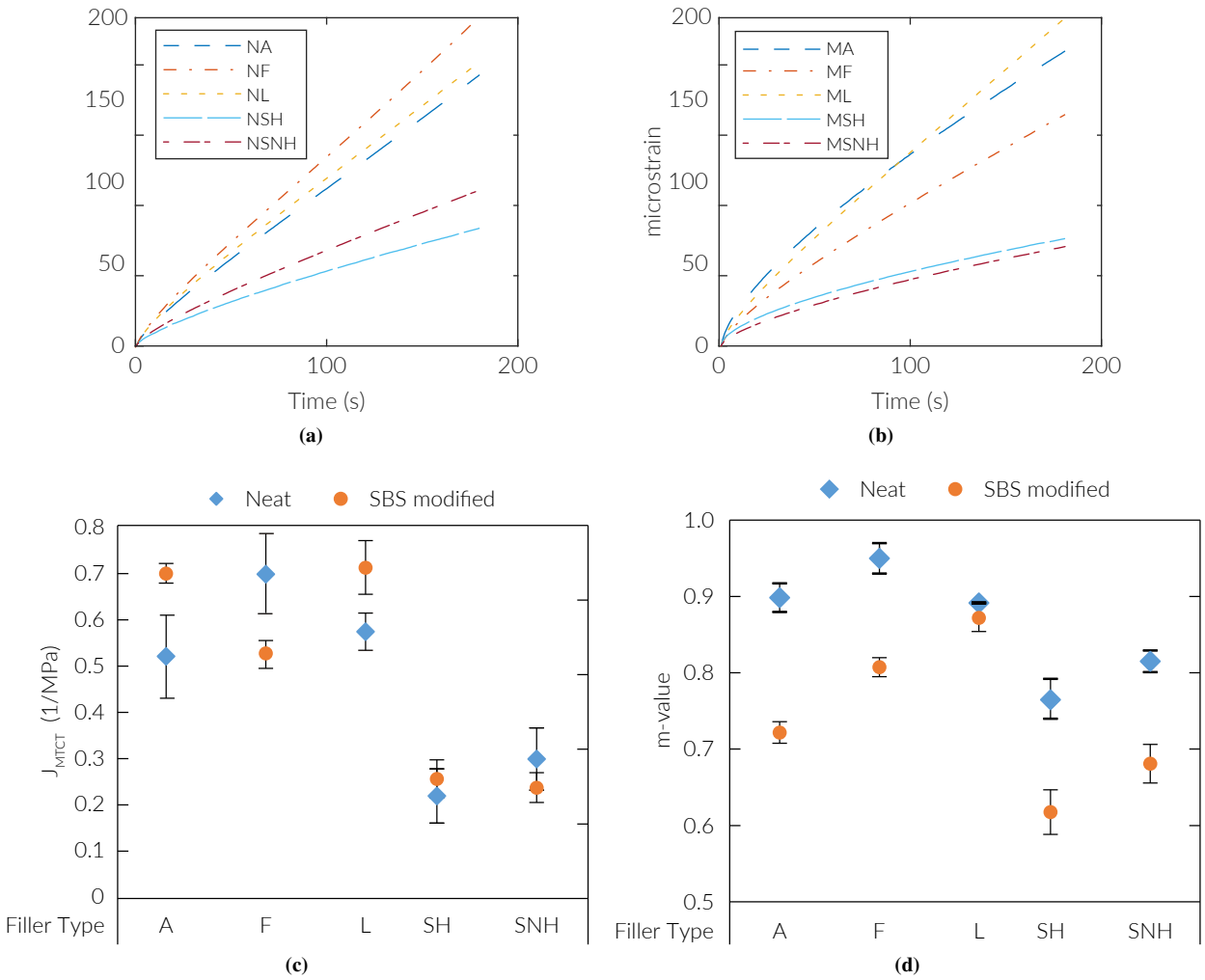

Figure 4. Results of the mastic analysis using the MTCT by Roberto et al. [20]. (**a**) and (**b**) show the strain curves for both the used asphalt binder used. The analysis in terms of J_{MTCT} and m-value is shown in (**c**), and (**d**).

terials coming from the steelmaking operation, as filler for the HMAs. Particularly, the effects of LFS hydration phenomenon were investigated by mineral and chemical analyses, involving XRF, XRD, and SEM-EDS investigations. Secondly, the LFS, hydrated and non-hydrated, were used to prepare HMA samples composed by two different asphalt binders, one neat and one SBS modified. The HMAs containing LFS were then compared to others prepared using three conventional fillers. The effects of the LFS hydration was evaluated at two different HMA-scales, mastic and HMA, using the recently-introduced MTCT (mastics) and the SuperPave (HMAs) protocols.

The results of the analyses performed provided the following findings:

- LFSs are mainly composed by silicates which exhibited no hydration effects. The huge presence of periclase (MgO) in all the samples show that hydration and consequently volumetric expansion does not occur for this phase. Therefore, despite the great presence of elemental Ca in the bulk material no lime (CaO) was found suggesting that Ca reacted very quickly hydrating (Portlandite) or forming silicates and aluminates.

- The use of the LFS in both mastics and HMAs increases the brittleness of the materials reducing the deformability. This important finding is likely due to both the presence of high content of hydrated lime and the fineness of grains. This effect was ex-

Table 4. Summary of the HMA SuperPave characterization results.

HMAs	M_R (GPa)	D(t) (1/GPa)	m-value	S_t (MPa)	ε_f (μstrain)
MA	18.47	0.86	0.45	3.32	1.09
MF	18.75	0.87	0.47	3.33	1.17
ML	16.12	1.30	0.38	3.01	1.00
MSH	14.52	1.36	0.40	2.89	0.95
MSNH	13.43	1.37	0.39	2.73	0.88
NA	14.66	1.38	0.40	2.74	0.79
NF	15.77	1.41	0.43	2.95	0.85
NL	17.80	2.05	0.56	3.56	0.73
NSH	17.55	1.90	0.55	3.39	0.72
NSNH	19.84	1.48	0.48	3.53	0.62

acerbated especially for the HMAs containing the non-hydrated LFS.

Future studies will focus on grain size investigation combining SEM-EDS and XRD analysis with the goal of determining the correct percentage of LFS to be used and the proper hydration method or procedure.

6. Acknowledgement

The Author wishes to thank Eng. Giovanni Bairo (Pittini Gorup) who provided the material and supported this research.

References

[1] Worldsteel ASSOCIATION, Steel - The permanent material in the circular economy, 2019. URL: https://www.worldsteel.org/.

[2] H. Motz, J. Geiseler, Products of steel slags an opportunity to save natural resources, Waste Management 21 (2001) 285–293. doi:10.1016/S0956-053X(00)00102-1.

[3] V. Ortega-López, J. M. Manso, I. I. Cuesta, J. J. González, The long-term accelerated expansion of various ladle-furnace basic slags and their soil-stabilization applications, Construction and Building Materials 68 (2014) 455–464. doi:10.1016/j.conbuildmat.2014.07.023.

[4] E. Bocci, Use of ladle furnace slag as filler in hot asphalt mixtures, Construction and Building Materials 161 (2018) 156–164. doi:10.1016/j.conbuildmat.2017.11.120.

[5] J. O. Akinmusuru, Potential beneficial uses of steel slag wastes for civil engineering purposes, Resources, Conservation and Recycling 5 (1991) 73–80. doi:10.1016/0921-3449(91)90041-L.

[6] J. Setién, D. Hernández, J. González, Characterization of ladle furnace basic slag for use as a construction material, Construction and Building Materials 23 (2009) 1788–1794. doi:10.1016/j.conbuildmat.2008.10.003.

[7] I. Z. Yildirim, M. Prezzi, Chemical, mineralogical, and morphological properties of steel slag, Advances in Civil Engineering 2011 (2011). doi:10.1155/2011/463638.

[8] C. Shi, S. Hu, Cementitious properties of ladle slag fines under autoclave curing conditions, Cement and Concrete Research 33 (2003) 1851–1856. doi:10.1016/S0008-8846(03)00211-4.

[9] M. Pasetto, A. Baliello, E. Pasquini, M. Skaf, V. Ortega-López, Performance-Based Characterization of Bituminous Mortars Prepared With Ladle Furnace Steel Slag, Sustainability 12 (2020) 1777. doi:10.3390/su12051777.

[10] M. Skaf, V. Ortega-López, J. Fuente-Alonso, A. Santamaría, J. Manso, Ladle furnace slag in asphalt mixes, Construction and Building Materials 122 (2016) 488–495. doi:10.1016/j.conbuildmat.2016.06.085.

[11] P. J. Rigden, The use of fillers in bituminous road surfacings. A study of filler-binder systems in relation to filler characteristics, Journal of the Society of Chemical Industry 66 (1947) 299–309. URL: http://doi.wiley.com/10.1002/jctb.5000660902. doi:10.1002/jctb.5000660902.

[12] M. Skaf, E. Pasquini, V. Revilla-Cuesta, V. Ortega-López, Performance and Durability of Porous Asphalt Mixtures Manufactured Exclusively with Electric Steel Slags, Materials 12 (2019) 3306. doi:10.3390/ma12203306.

[13] S. Choi, J.-M. Kim, D. Han, J.-H. Kim, Hydration properties of ladle furnace slag powder rapidly cooled by air, Construction and Building Materials 113 (2016) 682–690. doi:10.1016/j.conbuildmat.2016.03.089.

[14] V. S. Ramachandran, P. J. Sereda, R. F. Feldman, Mechanism of Hydration of Calcium Oxide, Nature 201 (1964) 288–289. doi:10.1038/201288a0.

[15] G. Wang, Y. Wang, Z. Gao, Use of steel slag as a granular material: Volume expansion prediction and usability criteria, Journal of Hazardous Materials 184 (2010) 555–560. doi:10.1016/j.jhazmat.2010.08.071.

[16] J. M. Montenegro, M. Celemín-Matachana, J. Cañizal, J. Setién, Ladle Furnace Slag in the Construction of Embankments: Expansive Behavior, Journal of Materials in Civil Engineering 25 (2013) 972–979. doi:10.1061/(ASCE)MT.1943-5533.0000642.

[17] S. Wu, Y. Xue, Q. Ye, Y. Chen, Utilization of steel slag as aggregates for stone mastic asphalt (SMA) mixtures, Building and Environment 42 (2007) 2580–2585. doi:10.1016/j.buildenv.2006.06.008.

[18] I. M. Asi, H. Y. Qasrawi, F. I. Shalabi, Use of steel slag aggregate in asphalt concrete mixes, Canadian Journal of Civil Engineering 34 (2007) 902–911. doi:10.1139/L07-025.

[19] E. Pasquini, G. Giacomello, M. Skaf, V. Ortega-Lopez, J. M. Manso, M. Pasetto, Influence of the Production Temperature on the Optimization Process of Asphalt Mixes Prepared with Steel Slag Aggregates Only, in: Lecture Notes in Civil Engineering, volume 48, 2020, pp. 214–223. doi:10.1007/978-3-030-29779-4_21.

[20] A. Roberto, E. Romeo, G. Tebaldi, A. Montepara, Introducing a new test protocol to evaluate the rate of damage accumulation in mastics at intermediate temperatures, Road Materials and Pavement Design (2021) 1–14. URL: https://doi.org/10.1080/14680629.2021.1906306. doi:10.1080/14680629.2021.1906306.

[21] R. Roque, W. G. Buttlar, Development of a measurement and analysis system to accurately determine asphalt concrete properties using the indirect tensile mode, Asphalt Paving Technology: Association of Asphalt Paving Technologists-Proceedings of the Technical Sessions 61 (1992) 304–332.

[22] W. G. Buttlar, R. Roque, Evaluation of empirical and theoretical models to determine asphalt mixture stiffnesses at low temper-

atures, Association of Asphalt Paving Technologists 65 (1996) 99–141.

[23] R. Roque, Z. Zhang, B. Sankar, Determination of Crack Growth Rate Parameters Of Asphalt Mixtures Using the Superpave IDT, Journal of the Association of Asphalt Paving Technologists 68 (1999) 404–433.

[24] R. Roque, B. Birgisson, B. Sangpetngam, Z. Zhang, Hot mix asphalt fracture mechanics: A fundamental crack growth law for asphalt mixtures, Journal of the Association of Asphalt Paving Technologist 71 (2002) 816–827.

[25] M. Pasetto, A. Baliello, G. Giacomello, E. Pasquini, Rheological characterization of warm-modified asphalt mastics containing electric arc furnace steel slags, Advances in Materials Science and Engineering 2016 (2016). doi:10.1155/2016/9535940.

[26] W. N. Findley, J. S. Lai, K. Onaran, Creep and Relaxation of Nonlinear Viscoelastic Materials - With an Introduction to Linear Viscoelasticity, 1976.

[27] R. J. Cominsky, H. Gerald A, T. W. Kennedy, M. Anderson, The superpave mix design manual for new construction and overlays (No. SHRP-A-407)., Technical Report, Washington, DC, USA, 1994.

[28] A. Gundla, S. Underwood, Evaluation of in situ RAP binder interaction in asphalt mastics using micromechanical models, International Journal of Pavement Engineering 18 (2015) 798–810. doi:10.1080/10298436.2015.1066003.

[29] A. Montepara, E. Romeo, M. Isola, G. Tebaldi, The Role of Fillers on Cracking Behavior of Mastics and Asphalt Mixtures, Journal of the Association of Asphalt Pavement Technologists 80 (2011) 161–191.

[30] G. D. Airey, Rheological properties of styrene butadiene styrene polymer modified road bitumens, Fuel 82 (2003) 1709–1719. doi:10.1016/S0016-2361(03)00146-7.

[31] E. Romeo, R. Roncella, S. Rastelli, A. Montepara, Mechanical influence of mineral fillers on asphalt mixture cracking behaviour, in: Asphalt Pavements - Proceedings of the International Conference on Asphalt Pavements, ISAP 2014, volume 1, 2014, pp. 903–911. doi:10.1201/b17219-111.

[32] C. V. Phan, H. Di Benedetto, C. Sauzéat, D. Lesueur, Influence of Hydrated Lime on Linear Viscoelastic Properties of Bituminous Mixtures, in: RILEM Bookseries, volume 11, Kluwer Academic Publishers, 2016, pp. 667–680. URL: http://link.springer.com/10.1007/978-94-017-7342-3{_}54. doi:10.1007/978-94-017-7342-3_54.

[33] J. Büchner, M. P. Wistuba, T. Hilmer, Creep Properties of Asphalt Binder, Asphalt Mastic and Asphalt Mixture, in: ISBM RILEM Symposium, 2020.

[34] A. Roberto, E. Romeo, A. Montepara, R. Roncella, Effect of fillers and their fractional voids on fundamental fracture properties of asphalt mixtures and mastics, Road Materials and Pavement Design 21 (2020) 25–41. URL: https://doi.org/10.1080/14680629.2018.1475297. doi:10.1080/14680629.2018.1475297.

[35] W. H. Goetz, L. E. Wood, Bituminous Materials and Mixtures, in: Section 18: Highway Engineering Handbook , Woods, K. B. , ed., McGraw- Hill, New York, 1960.